Available online at www.sciencedirect.com
SCIENCE DIRECT®
ELSEVIER
Nuclear Instruments and Methods in Physics Research A 531 (2004) 75–81
NUCLEAR INSTRUMENTS & METHODS IN PHYSICS RESEARCH
Section A
www.elsevier.com/locate/nima

Intrinsic spatial resolution of semiconductor X-ray detectors: a simulation study

M. Hoheisel[a,*], J. Giersch[b], P. Bernhardt[a]

[a] Siemens AG Medical Solutions, Siemensstr. 1, D-91301 Forchheim, Germany
[b] Physics Institute University Erlangen Nürnberg, Erlangen, Germany

Available online 11 June 2004

Abstract

We have investigated the intrinsic limitation of the spatial resolution of a directly absorbing semiconductor detector. The primary interaction of an incident X-ray quantum is followed by a series of processes that generate Compton or fluorescence photons and subsequent electrons. Their ranges determine the spatial resolution of the detector, expressed in terms of the modulation transfer function. The effects of carrier transport have been neglected in this work.

Monte Carlo simulations have been carried out in the 10–100 keV energy range with the program, ROSI (Roentgen Simulation), which is based on the well-established EGS4 algorithm. On a fine grid, the lateral distribution of deposited energy has been calculated in typical materials such as Se, CdTe, HgI_2 and PbI_2. The results can be used to either determine the point spread function of an energy-integrating detector, or to study multiple registration in adjacent pixels of photon-counting detectors.

The results show that the complex absorption process determines the spatial resolution of the detector considerably. If a very high spatial resolution is required, a well-adapted semiconductor should be applied. Dependent on the energy range used, lists of favorable materials are given. At energies above 50 keV, Compton scattering reduces spatial resolution in the high frequency range.

PACS: 29.40.Wk; 32.80.−t; 72.20.Jv; 87.57.Ce

Keywords: Medical X-ray imaging; Detectors; Absorber; Photon counting; Monte Carlo simulation; Modulation transfer function

1. Introduction

In the field of medical X-ray detectors, semiconductor-based flat-panel detectors have begun to replace conventional film-screen systems, storage phosphor plates, or image intensifier TV systems. Directly absorbing semiconductors are an attractive alternative to the scintillator plus photodiode concept. The detectors consist of matrices of switches made from amorphous silicon thin-film transistors, coupled to either photodiodes to register the scintillation light, or a semiconductor layer [1]. The signal is integrated over the pixel area, but photon counting is also feasible.

*Corresponding author. Siemens AG, Basic Development, Medical Engineering, P.O. Box 3260, Erlangen 91050, Germany. Tel.: +49-9191-18-9703; fax: +49-9191-18-8951.
E-mail address: martin.hoheisel@siemens.com (M. Hoheisel).

0168-9002/$ - see front matter © 2004 Elsevier B.V. All rights reserved.
doi:10.1016/j.nima.2004.05.077

Directly absorbing semiconductors exhibit an excellent spatial resolution even in relatively thick layers (e.g. 500 μm) because radiation-generated secondary charge carriers have a lateral diffusion length which is small compared to their drift length. Moreover, spatial resolution is limited by intrinsic processes associated with X-ray scattering and absorption as well as energy loss of the generated electrons [2].

Of course, the results have to be seen with respect to the requirements for medical X-ray detectors. For the imaging of soft tissue, resolutions of 0–2 lp/mm (line pairs per mm) are mandatory. For bones, even more than 3 lp/mm are favorable, and special applications such as dental radiography or mammography require >5 lp/mm up to 10 lp/mm [3].

2. Simulations

The signal-generating processes have been studied by Monte Carlo simulations using the program, ROSI (Roentgen Simulation) written by Giersch et al. [4]. Since the energy range relevant for medical diagnosis lies between 10 and 100 keV, several energies have been selected in this interval and monochromatic simulations have been carried out.

The first simulation step is the X-ray interaction of the incident radiation with the absorber. Quanta can become elastically scattered (Raleigh scattering), inelastically scattered (Compton scattering) where the quanta loose energy and fast electrons are generated, or absorbed by photoelectric process where fluorescence quanta and also fast electrons are generated. The secondary quanta travel a certain distance and either leave the absorber or interact in a consecutive process. Thus, X-ray absorption takes place in a distributed manner in space.

The second simulation step is the energy loss of the fast electrons. They can be elastically or inelastically scattered. In the latter process, multiple electron–hole pairs are excited. Thus, electron energy loss is also a process which leads to a signal generation distributed in space.

The excited charge carriers, in the case of a directly absorbing semiconductor, are collected by an electrical drift field. Moreover, carrier diffusion tends to distribute the signal in space. The ratio of diffusion length to drift length is relevant to tell how the signal is blurred by charge transport. In our simulations, we neglected this effect. We will include it in future investigations.

The signal is collected in a pixel, i.e. the signal is integrated over the active pixel area. In terms of modulation transfer function, the pixel size determines a sinc function ($\sin(x)/x$) as an upper limit for an ideal detector. The signal is finally made ambiguous through the discrete sampling for spatial frequencies above the Nyqvist frequency.

In the simulations an X-ray fan beam is directed onto the detector that is assumed to consist of a 10-μm wide pixel grid. The beam is slightly tilted (by 5°) to produce oversampling. An example for a resulting image is given in Fig. 1. From this image, we determine the line spread function which is shown in Fig. 2 on a linear scale. Replotting it on a logarithmic scale (Fig. 3) unravels a narrow and a broad component which is a sign of two different underlying processes.

Finally, the modulation-transfer function (MTF) was calculated (Fig. 4) [5]. It exhibits a

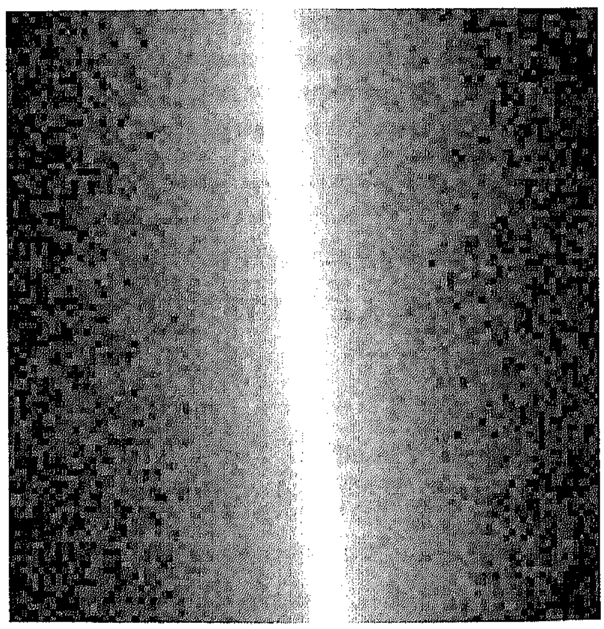

Fig. 1. Simulated image of an infinitesimal thin X-ray fan beam, 100 keV, on a 600 μm thick CdTe detector. Pixel size is 10 μm.

continuous decay from 100% at 0 lp/mm down to 30% at 30 lp/mm. Above 50 lp/mm it flattens out. The sinc function

$$\mathrm{sinc}(10\,\mu\mathrm{m\,f}) = \frac{\sin(10\,\mu\mathrm{m}\,\pi\mathrm{f})}{10\,\mu\mathrm{m}\,\pi\mathrm{f}}$$

for the chosen pixel size of 10 μm is plotted for comparison. It marks the theoretical upper limit for the MTF.

Several different materials have been investigated, namely the elementary semiconductors Si, Ge and Se, compounds as GaAs, CdTe, HgI_2, PbO and PbI_2, and the scintillators Gd_2O_2S and CsI. The layer thicknesses were 200 μm for the mammography energy range (10–25 keV), and 600 μm for radiography (31–100 keV).

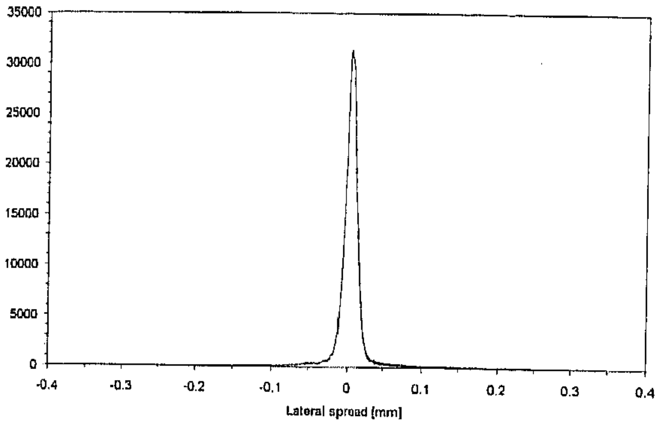

Fig. 2. Line spread function of the image of Fig. 1 on a linear scale.

3. Results

To explain the most important features, some selected curves will be shown. In Fig. 5 the MTF in the mammographic energy range is plotted for CdTe. All curves are close to the sinc function. It should be mentioned that in this case the energies investigated are below the K-edge energies of Cd and Te, which are 26.7 and 31.8 keV, respectively. Another example is Se (Fig. 6) with a K-edge of 12.7 keV. Here the MTF curve directly above the K-edge energy (13 keV) is the lowest while with increasing energy the curves rise again.

In Fig. 7 the MTF in the radiographic energy range is plotted for CdTe. Here the MTF decreases for all curves, but the strongest decrease is found at 34 keV directly above the K-edge energies. At higher energies, this decrease is less pronounced. Above 70 keV a second effect can be seen. At higher spatial frequencies (>20 lp/mm) the MTF shows a strong decay. Since in the case of Se all curves are above the K-edge energy (Fig. 8), a high-frequency drop is only found above 50 keV.

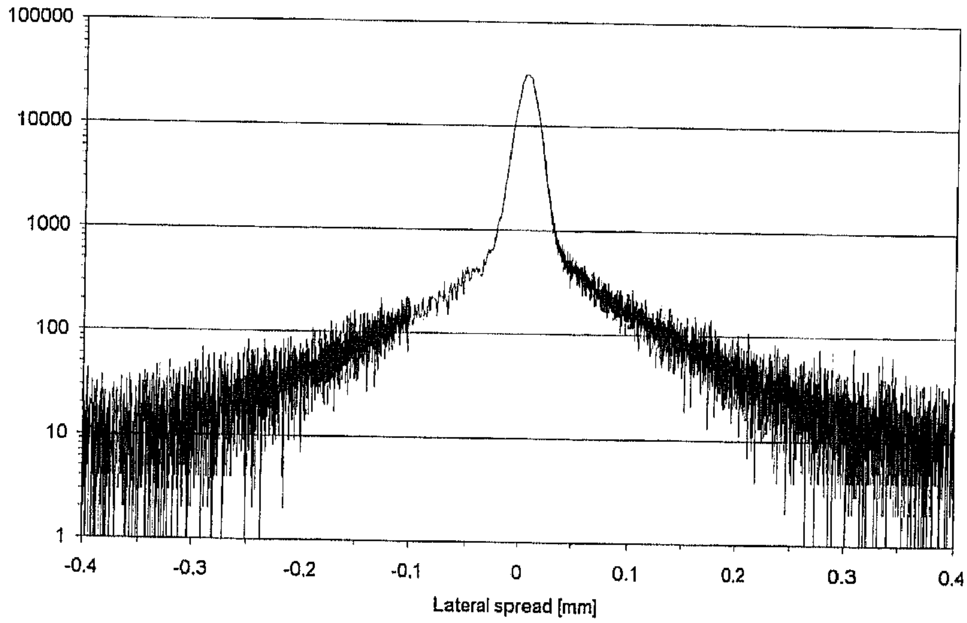

Fig. 3. Line spread function of Fig. 2 on a logarithmic scale. A narrow and a broad component indicate two different processes.

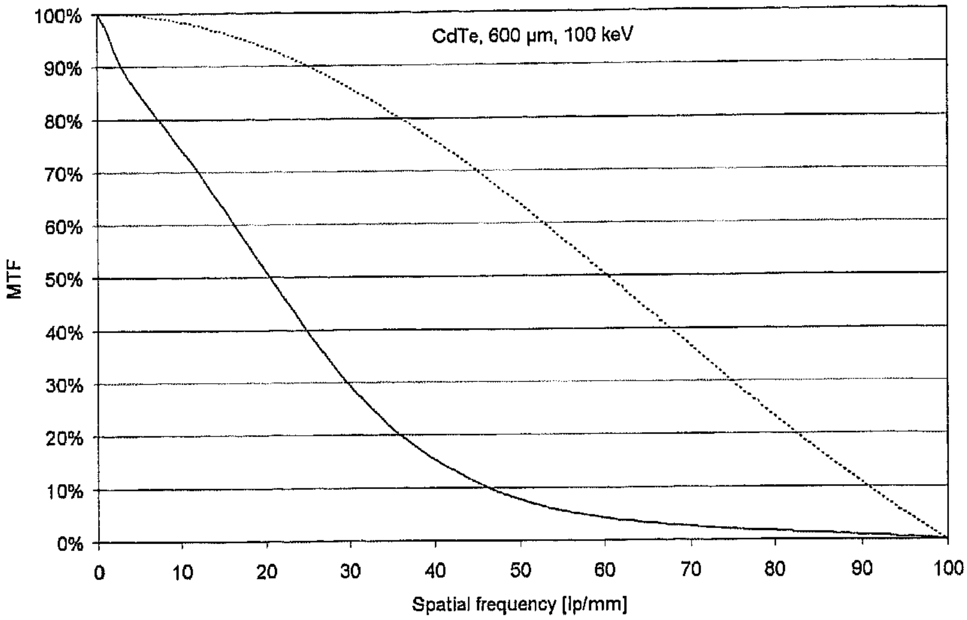

Fig. 4. MTF determined from the line spread function of Fig. 2 compared with the sinc function (dotted line).

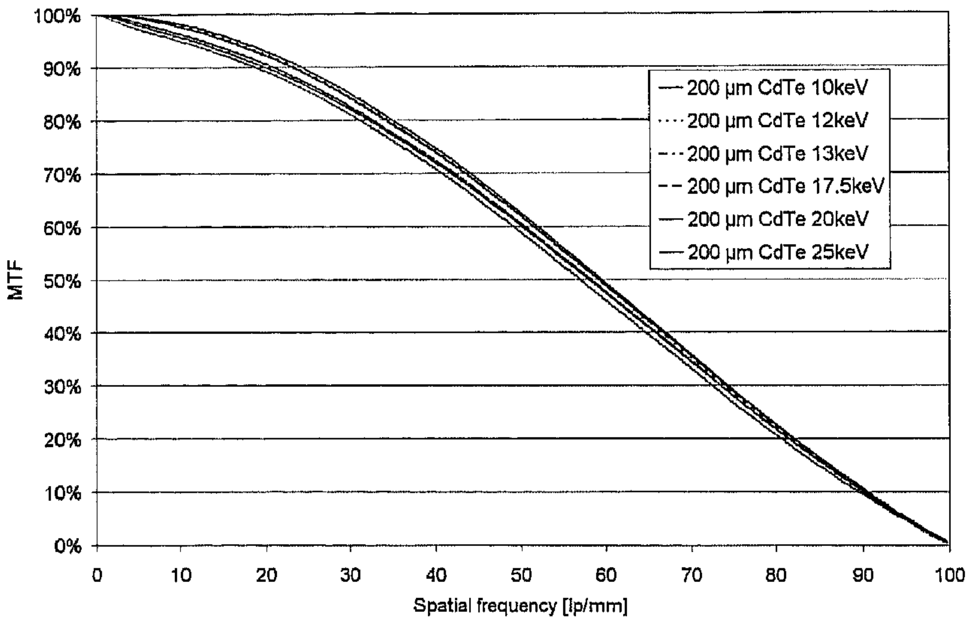

Fig. 5. MTF of a 200 µm thick CdTe detector in the mammographic energy range (10–25 keV). All curves are close to the sinc function.

All data from the other absorber materials not displayed here show more or less the same features. At X-ray energies below the K-edge energy the curves run close to the sinc function. At energies above the K-edge energy, the curves start to decrease even at lower spatial frequencies. This can be attributed to K-fluorescence where reabsorption may take place some 100 µm away from the initial interaction site. This effect spreads the signal in space, thus reducing the MTF.

At even higher energies, i.e. 50 keV, the MTF becomes rather low above 20 lp/mm. The origin of this behavior is the Compton effect. Compton scattered quanta have much lower energies

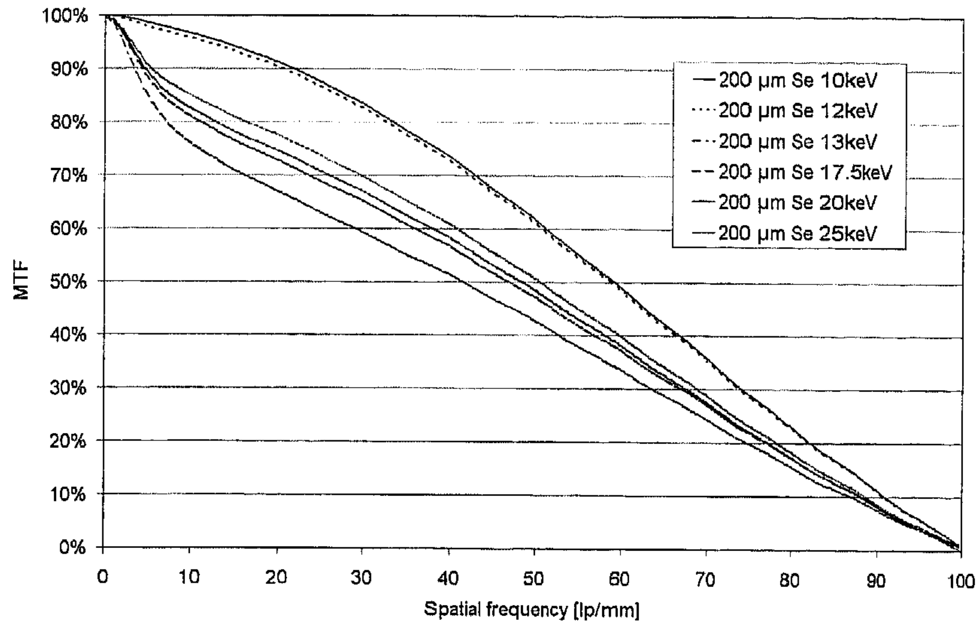

Fig. 6. MTF of a 200 μm thick Se detector in the mammographic energy range (10–25 keV). At 10 and 12 keV, curves are close to the sinc function, at higher energies they exhibit a drop.

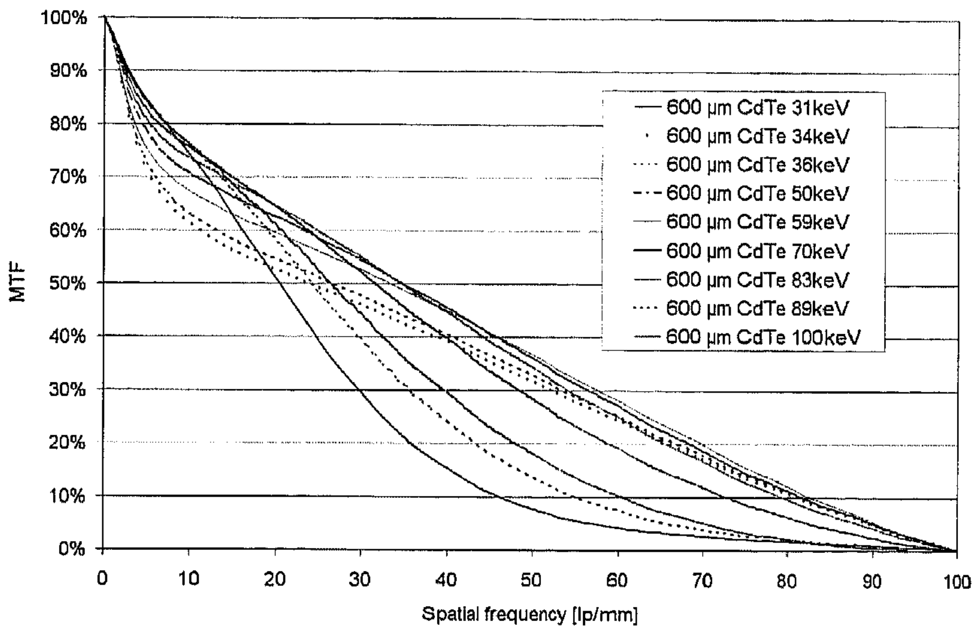

Fig. 7. MTF of a 600 μm thick CdTe detector in the radiographic energy range (31–100 keV). Above 70 keV the high spatial frequency (>20 lp/mm) MTF drops considerably.

compared to the incident quanta. Therefore, they become absorbed in the vicinity of the first interaction. Hence only the high-frequency MTF is affected.

Since the diagrams (Fig. 5–8) are rather complex, Fig. 9 shows a cross-section through all curves at a constant spatial frequency. The MTF is plotted at 10 lp/mm as a function of X-ray energy. At the top of the diagram, dashes mark the positions of the chemical elements involved. All curves show a sharp decrease at the K-edges, but increase again at higher energies. The reason for this increase is that more energy becomes transferred to electrons compared to the fluorescence

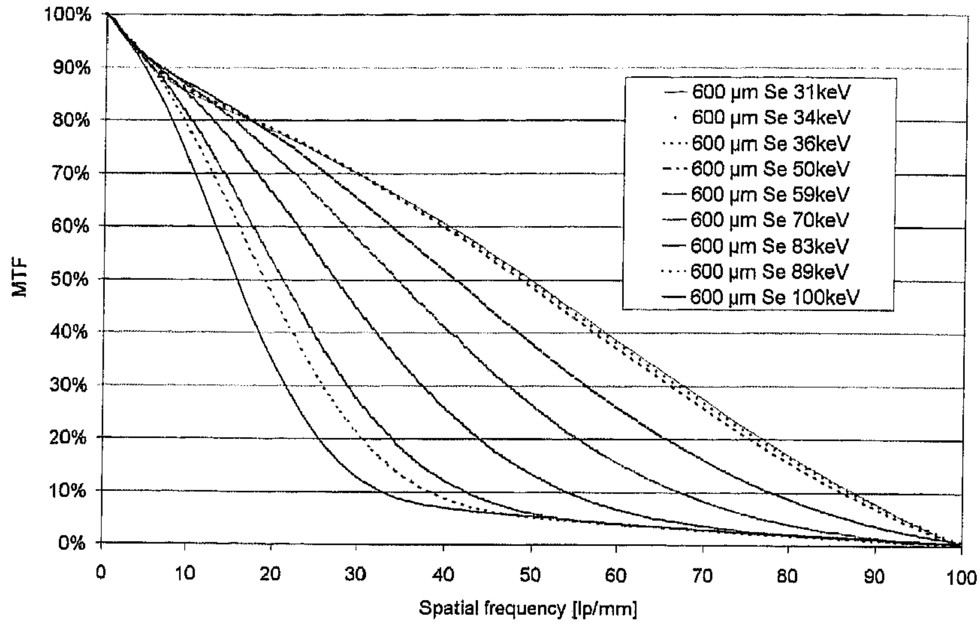

Fig. 8. MTF of a 600 µm thick Se detector in the radiographic energy range (31–100 keV).

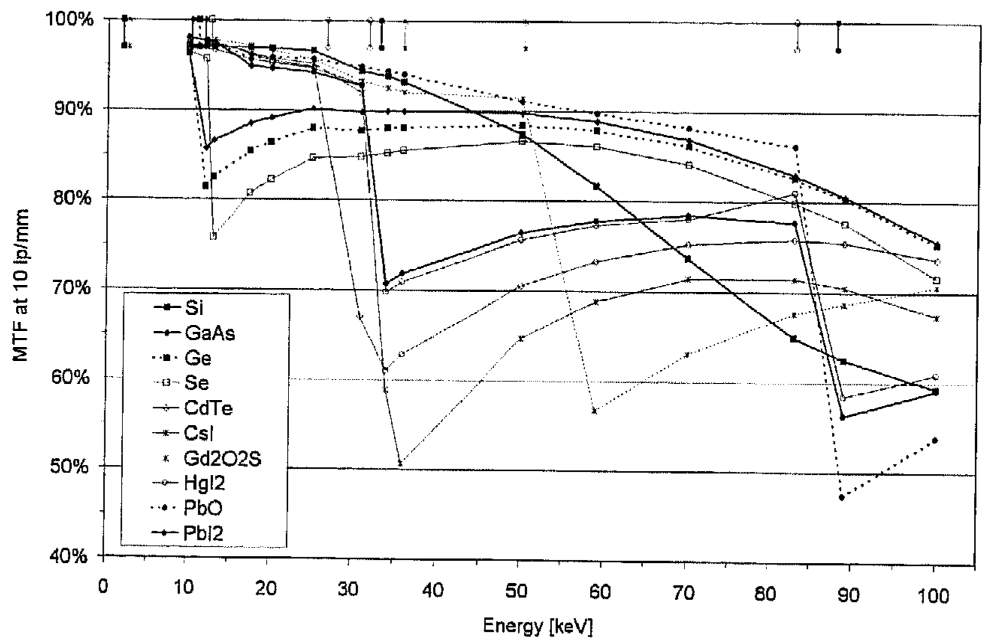

Fig. 9. MTF vs. energy of all materials investigated at 10 lp/mm. The K-edge energies are marked at the top of the diagram by small dashes. All curves show a sharp decrease at the K-edges, but increase again at higher energies.

quanta and is thus absorbed near the locus of incidence.

4. Conclusions

If for a specific application a detector with high spatial resolution is required, the absorber material should be adapted to the X-ray spectrum used. The maximum of the spectrum is to be placed at an energy where the MTF of the favored absorber is high.

The most common detector materials, such as cesium iodide and selenium, operate far from fundamental spatial resolution limits. Only if extremely high resolutions far beyond today's mammography and radiography applications are required, other absorbers might be advantageous.

Our simulations with monochromatic X-rays lead to the conclusion that for mean energies around 20 keV, CdTe, CsI, Gd_2O_2S, HgI_2, PbO and PbI_2 provide the highest MTF. For 40–80 keV, GaAs, Ge, Se and PbO yield the best MTF.

It has to be pointed out that the simulations have been carried out up to 100 lp/mm. The relevant spatial frequencies for medical diagnosis are much lower (0–5 lp/mm, see above). Therefore, the MTF reduction found in this investigation can be tolerated in many cases.

An interesting observation is that the strongest MTF decrease is found just above the K-edge, i.e. at an energy where the absorption has its highest value. This has a strong influence on the selection of the absorber material. In most cases, high absorption is more important than high spatial resolution. Every percent of additional absorption allows the reduction of the radiation dose for a diagnostic procedure. A slightly reduced MTF can be borne in the majority of cases.

Acknowledgements

This work has been supported by the BFS (Bavarian Science Foundation).

References

[1] M. Hoheisel, M. Arques, J. Chabbal, C. Chaussat, T. Ducourant, G. Hahm, H. Horbaschek, R. Schulz, M. Spahn, J. Non-Cryst. Solids 227–230 (1998) 1300.

[2] G. Hajdok, J.J. Battista, I.A. Cunningham, Proc. SPIE 5030 (2003) 1.

[3] M. Hoheisel, L. Bätz, Thin Solid Films 383 (2001) 132.

[4] J. Giersch, A. Weidemann, G. Anton, Nucl. Instr. and Meth. A 509 (2003) 151.

[5] I.A. Cunningham, B.K. Reid, Med. Phys. 19 (1992) 1037.